

Communication

Microstructure and Strength of NiTi-Nb Eutectic Braze Joining NiTi Wires

LIQIANG WANG, CONG WANG, and DAVID C. DUNAND

NiTi wires were brazed together *via* liquid eutectic formation between NiTi and Nb powders deposited at the wire contact region. The brazed region shows proeutectic NiTi(Nb) in contact with the wires, sandwiching a NiTi-Nb eutectic structure, whose microhardness and stiffness, as characterized *via* nanoindentation, are higher than the NiTi wires, while also showing signs of high ductility. NiTi-Nb eutectic bonding may thus be a viable approach for producing shape-memory NiTi scaffolds brazed from stacked, woven, or braided wires.

DOI: 10.1007/s11661-015-2781-z

© The Minerals, Metals & Materials Society and ASM International 2015

NiTi alloys are widely used in the biomedical field because of their excellent shape-memory effect and superelasticity, low stiffness, and good biocompatibility.^[1-3] Porous NiTi alloys further have excellent potential for osseointegration, reducing stress concentrations at the bone/implant interface under load-bearing conditions.^[4,5] However, NiTi foams with random pores exhibit lower strength, stiffness, and permeability than NiTi with spatially ordered porosity or channels. One example of the latter type of structures is NiTi honeycombs with low density and good shape memory developed toward biomedical applications.^[6-8] NiTi truss structures have also been fabricated in a number of geometries by 3D additive manufacturing.^[9] An alternate method is to use wires to create 3D lattice structures, as demonstrated by Kang *et al.* with various helical metal wires (but not NiTi)^[10-12] or by Fonda *et al.* with woven flexible copper wires.^[13] To achieve high strength and stiffness in such woven, braided, or assembled metal wire structures, it is necessary to bond the wires at their contact points. This is achieved by depositing brazing paste at each successive contact point

during the wire assembly process,^[12] or by concentrating solder powders at the wire junctions by dipping the woven structure in a powder slurry.^[13]

For NiTi, a particularly interesting braze is the NiTi-Nb eutectic, as Nb is biocompatible, does not embrittle NiTi nor decreases its shape-memory capability, except for an increase in the shape-memory hysteresis.^[14,15] When pure NiTi and Nb are in contact with each other, a quasi-binary liquid eutectic phase with composition near Ni-36Ti-26Nb (at. pct) forms at 1453 K (1180 °C).^[6,7] Grummon *et al.* used Nb foils to bond by this method NiTi foils into open-cell NiTi honeycombs with shape-memory properties.^[6] Bansiddhi and Dunand used the liquid NiTi-Nb eutectic phase to bond NiTi powders and create porous NiTi.^[16,17]

In this paper, we demonstrate how the liquid NiTi-Nb eutectic can be used to braze NiTi wires, rather than NiTi powders or foils as in previous work.^[6,16,17] The mixture of NiTi powder and Nb powder is used here to braze NiTi wires *via* an *in situ* reaction process, thus opening the door to bonding of woven, braided, or assembled NiTi wire structures. The microstructure, micro-hardness, and stiffness of the eutectic phase are reported, and the interface between the solid NiTi wires and the solidified NiTi-Nb eutectic braze is examined.

Annealed commercial-grade NiTi wires with a nominal composition of 50.5 at. pct Ni and a diameter of 300 μm were obtained from Xi'an Saite Metal Materials Development (China). The wires were polished to remove surface oxides and cut to length of 10 mm. An automatic polishing machine outfitted with sandpaper and polishing cloth was used to remove surface oxides. Pre-alloyed NiTi powders (44 to 63 μm , 48.6 at. pct Ni, Special Metals Corp., NY) and pure Nb powders (99.8 pct purity, 1 to 5 μm , Alfa Aesar, MA) were used, together with polyvinyl alcohol PVA (87 to 89 pct hydrolyzed, high molecular weight, from Alfa Aesar, MA).

Five steps were carried out to bond the NiTi wires: (i) blend 0.5 g NiTi and Nb powder (with weight ratio 1:1, less than the weight ratio 1.6:1 for the eutectic phase) and tumble for 2 hours; (ii) add the NiTi/Nb powder blend and 0.04 g PVA to 0.6 mL H₂O to create a slurry; (iii) deposit slurry at contact area between two parallel, partially overlapping NiTi wires using a syringe; (iv) remove water and PVA by heating at 523 K (250 °C) for 1 hour in air; (v) melt the NiTi/Nb powders by heating to 1453 K (1180 °C) (above the 1443 K (1170 °C) eutectic temperature in the NiTi-Nb quasi-binary phase diagram^[6,18]) and maintain the liquid eutectic at that temperature for 8 minutes to bond the wires in a high vacuum (10⁻⁵ torr) furnace with pure titanium getters.

SEM observations were carried out using a Hitachi SU8030 microscope at 15 kV. Nanoindentation experiments were performed using a nanomechanical test system with a Berkovich tip, which was controlled up to a maximum load of 50 mN with a loading rate of 1.0 mN/s. Before the unloading step performed at a rate of 1.0 mN/s, a 30 seconds dwelling time was applied at the maximum load. The distance between individual indents was programmed to be 15 μm . The Oliver-Pharr method was used to calculate the nanohardness and Young's modulus of the indented material.^[19]

LIQIANG WANG, Associate Professor, is with the State Key Laboratory of Metal Matrix Composites, Shanghai Jiao Tong University, Shanghai 200240, P.R. China, and also with the Department of Materials Science & Engineering, Northwestern University, Evanston, IL 60208. Contact e-mail: wang_liqiang@sjtu.edu.cn
CONG WANG, Professor, formerly with the Department of Materials Science & Engineering, Northwestern University, is now with the School of Materials and Metallurgy, Northeastern University Shenyang 110819, P.R. China. DAVID C. DUNAND, Professor, is with the Department of Materials Science & Engineering, Northwestern University. Contact e-mail: dunand@northwestern.edu

Manuscript submitted March 13, 2014.

Article published online February 11, 2015

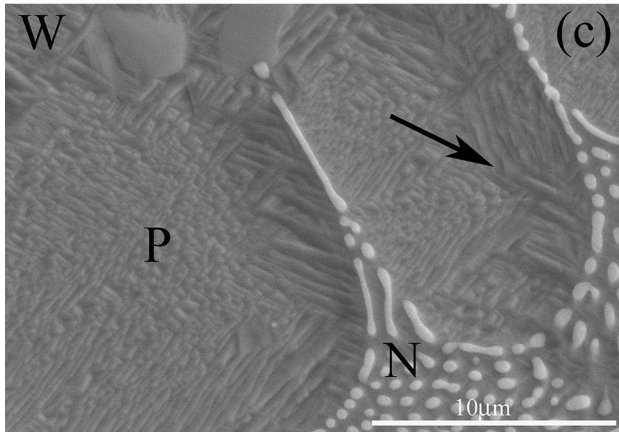
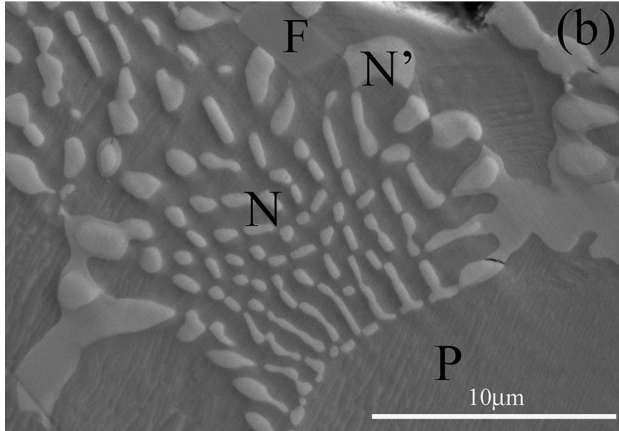
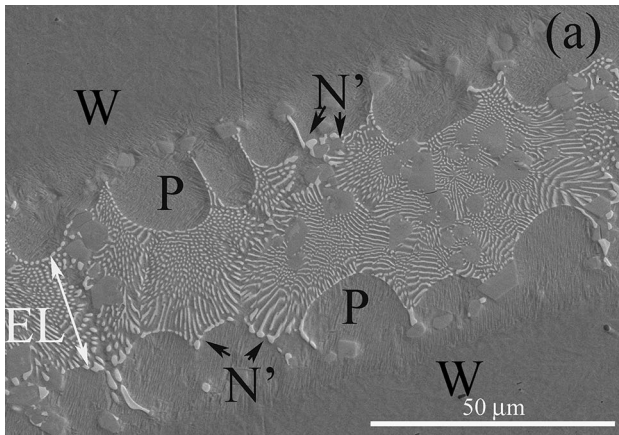


Fig. 1—SEM micrographs of polished surface of the brazed region: (a) Solidified braze joining two NiTi wires (W) showing an EL and proeutectic NiTi(Nb) phase (P) with Nb-rich particles (N'); (b) Eutectic consisting of Nb (N) rods (light color) within a NiTi matrix, Ti-rich faceted particles (F), in contact with proeutectic NiTi(Nb) phase (P) and Nb-rich particles (N'); (c) interface between eutectic with rod-like Nb phase (N) and proeutectic NiTi(Nb) phase (P).

Figures 1(a) through (c) show SEM micrographs of the as-polished surface of the brazed region between two NiTi wires, where 10 mg NiTi/Nb powder mixture was used. As demonstrated in Figure 1(a), the width of the bonding layer between the wires is about $\sim 50 \mu\text{m}$. It consists of a $\sim 25 \mu\text{m}$ wide eutectic layer (EL) sandwiched by two layers of rounded proeutectic (or primary) NiTi(Nb) phase (P) in contact with the NiTi

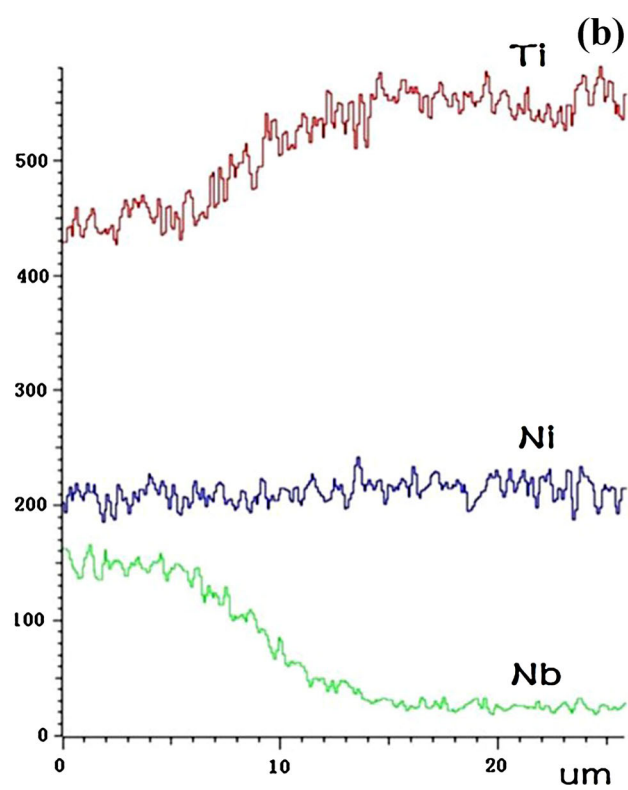
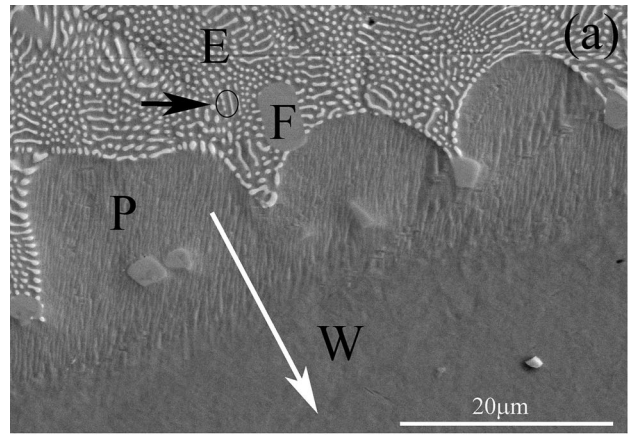


Fig. 2—(a) SEM micrographs of polished braze region showing eutectic (E), proeutectic NiTi(Nb) phase (P), NiTi wire (W) and faceted Ti-rich particles (F); (b) Composition profile (arbitrary units), measured over white line in (a) from proeutectic phase (P) to wire (W).

wires (W). Particles of an additional Nb-rich phase (N') are also present at the interface between the wire (W) and the proeutectic phase (P), as well as within the EL. As shown in Figure 1(b), the eutectic Nb phase (N) consists of fine rods, with submicron width, within a NiTi matrix. Ti-rich particles are observed in the form of discrete, faceted particles (F). Figure 1(c) shows surface relief typical of martensitic transformation within the proeutectic NiTi(Nb) phase (P), whose composition as measured by EDS analysis (arrow in Figure 1(c)) is Ni-43Ti-8Nb (at. pct). The presence of Nb in this phase is a strong indication that these regions are proeutectic

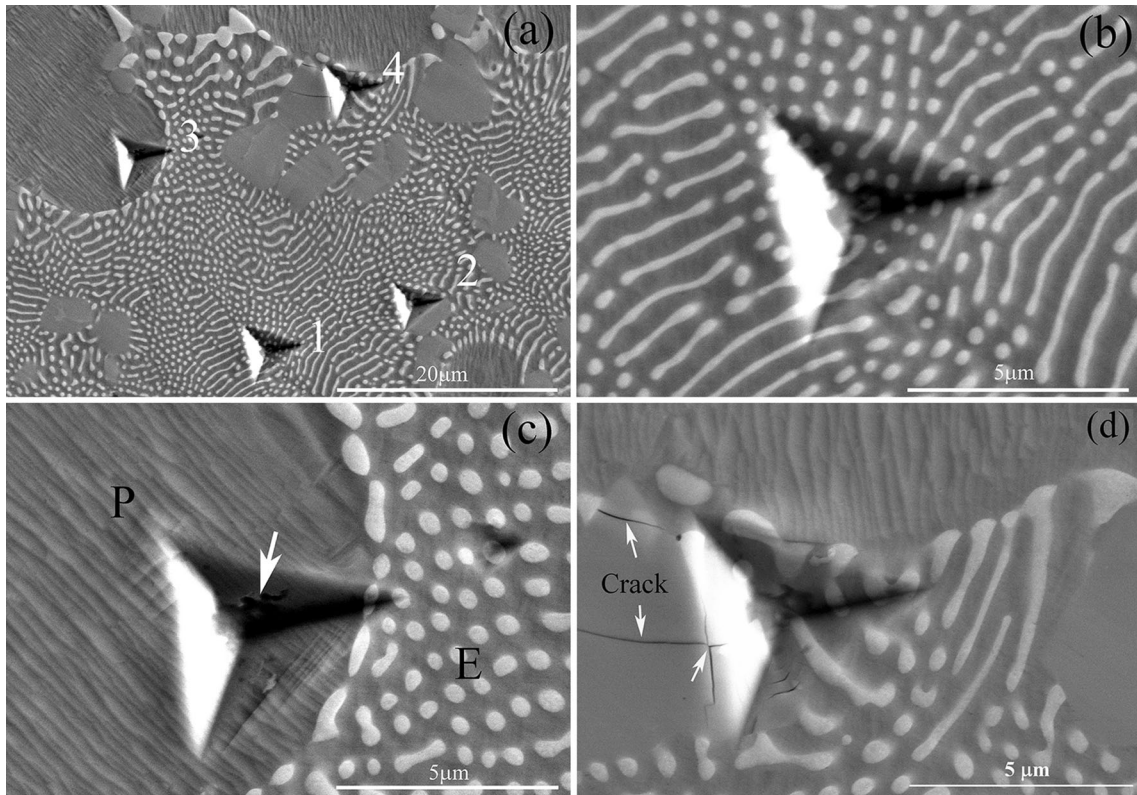


Fig. 3—SEM micrographs of polished brazed region and NiTi wire with nanoindents. (a) Four indents (labeled 1 to 4) shown at low magnification. (b) High magnification image of indent 1 in rod-like eutectic phase. (c) High magnification image of indent 3 in proeutectic NiTi(Nb) phase (P) with one corner impinging on the interface with the rod-like eutectic (E). (d) High magnification image of indent 4 in Nb-rich particle and rod-like eutectic phase.

phases solidified onto the wire prior to eutectic solidification, not part of the eroded NiTi wire or original NiTi powders. Similar observations were made in References 6 and 7.

Figure 2 shows another SEM micrograph of the brazed region between two NiTi wires. Nb concentration is high in the proeutectic NiTi(Nb) phase and near zero in the wires, showing that solid-state diffusion of Nb into the wires is very limited during the 8 minutes of contact time between the liquid eutectic and the wires at 1453 K (1180 °C). The Ni content is constant along the profile, showing that Nb replaces Ti upon solidification of the proeutectic phase. As measured by EDS in Figure 2(a), the composition of the eutectic is Ni-39Ti-25Nb (at. pct), close to the quasi-binary eutectic composition of Ni-36Ti-26Nb (at. pct) reported in References 6 and 7.

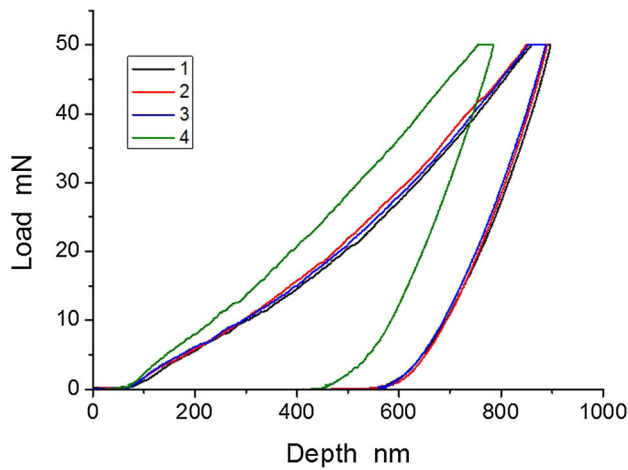
Figure 3 shows the SEM images of nanoindents on polished surface. Figure 3(a) indicates four nanoindents in the EL and the proeutectic NiTi(Nb) phase. Ductile behavior of the eutectic region can be inferred from the smooth, crack-free indent in Figure 3(b). Lack of cracks at the corners of the indent in Figure 3(c) also implies ductile behavior in the proeutectic phase (P) and at the interface between the proeutectic phase and the eutectic region (E). Small fracture features are, however, visible in Figure 3(c) at the bottom of the indent within the

proeutectic phase. As for the Nb-rich particle near the proeutectic phase, several linear cracks appear on the boundary of particle and rod-like eutectic phase and extend to the particle, as indicated in the high magnification in Figure 3(d). The ductile property varies from the morphology in the eutectic region and rod-like eutectic phase shows excellent ductile characterization.

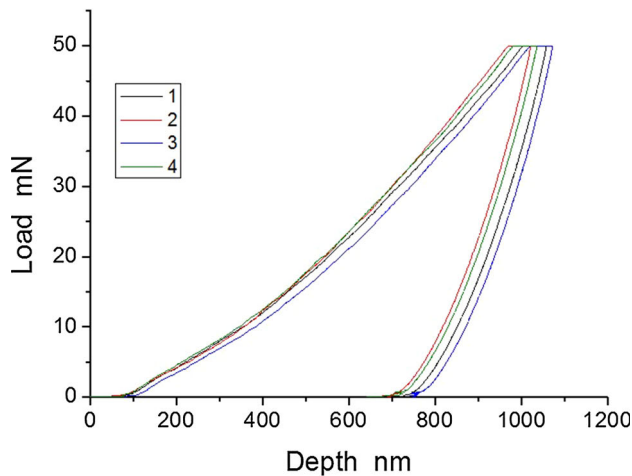
Figure 4(a) shows load/unload–displacement curves for the indents in the bonding layer shown in Figure 3(a), which display a maximum depth of ~900 nm for the indents (1) to (3) and <800 nm for indent (4). Figure 4(b) shows the load/unload–displacement curves for four indents created in the NiTi wire: the maximum depth is close to 1000 nm, which indicates that the wires are softer than the bonding layer.

Stabilized dynamic hardness values of the four indents (1) to (4) in the bonding layer shown in Figure 4(a) are 3.9, 4.1, 4.0, and 5.5 GPa, respectively. The value of the hardness is a clear evidence for the observation of nanoindents in Figure 3 and Ti-rich particle shows highest hardness in eutectic region. By contrasts, the hardness values measured on the NiTi wire are 2.6, 3.0, 2.6, and 2.9 GPa, with an average of 2.8 GPa which is significantly lower than the hardness of the bonding layer (4.0 GPa, when averaging the first three measurements).

The stabilized stiffness values for the four indents (1) to (4) in the bonding layer are 67.5, 67.6, 68.4, and



(a)



(b)

Fig. 4—Load–displacement plots during nanoindentation experiments in (a) the bonding layer (numbers correspond to indents shown in Fig. 3(a)), (b) a NiTi wire.

75.5 GPa, respectively, which are again higher than those for the NiTi wire (62.6, 57.9, 58.1, and 57.2 GPa). The latter values are close to the Young's modulus of 58 GPa reported for bulk NiTi along the $\langle 111 \rangle$ direction.^[20]

In summary, melting at 1453 K (1180 °C) of a blend of NiTi and Nb powders placed between two NiTi wires creates a bonding region consisting of proeutectic NiTi(Nb) phase and NiTi-Nb eutectic. Nanoindentation of the bonding region indicates high ductility, together with hardness and stiffness that are higher than those of

the NiTi wires. This brazing method may thus be a viable approach for bonding NiTi wires in assembled or woven scaffolds with shape-memory properties.

This research was supported by DARPA under the Grant W91CRB1010004. National Science Foundation under Grant No: 51302168 of China. The authors gratefully acknowledge experimental hardness measurements by Dr. Lechun Xie from Shanghai Jiao Tong University.

REFERENCES

1. L.G. Machado and M.A. Savi: *Braz. J. Med. Biol. Res.*, 2003, vol. 36 (6), pp. 683–91.
2. A. Biesiekierski, J. Wang, M.A.H. Gepreel, and C. Wen: *Acta Biomater.*, 2012, vol. 8 (5), pp. 1661–69.
3. Y.P. Zhang, D.S. Li, and X.P. Zhang: *Scripta Mater.*, 2007, vol. 57 (11), pp. 1020–23.
4. A. Bansiddhi, T.D. Sargeant, S.I. Stupp, and D.C. Dunand: *Acta Biomater.*, 2008, vol. 4 (4), pp. 773–82.
5. X.M. Liu, S.L. Wu, K.W.K. Yeung, Y.L. Chan, T. Hu, Z.S. Xu, X.Y. Liu, J.C.Y. Chung, K.M.C. Cheung, and P.K. Chu: *Biomater.*, 2011, vol. 32 (2), pp. 330–38.
6. D.S. Grummon, J.A. Shaw, and J. Foltz: *Mater. Sci. Eng. A*, 2006, vols. 438–440, pp. 1113–18.
7. D.S. Grummon, J.A. Shaw, and A. Gremillet: *J. Appl. Phys. Lett.*, 2003, vol. 82 (16), pp. 2727–29.
8. P.A. Michailidis, N. Triantafyllidis, J.A. Shawa, and D.S. Grummon: *Int. J. Solids Struct.*, 2009, vol. 46 (13), pp. 2724–38.
9. H.N.G. Wadley, N.A. Fleck, and A.G. Evans: *Compos. Sci. Technol.*, 2003, vol. 63 (16), pp. 2331–43.
10. J.S. Park, J.H. Joo, B.C. Lee, and K.J. Kang: *Int. J. Mech. Sci.*, 2011, vol. 53 (1), pp. 65–73.
11. K.J. Kang: *Acta Mater.*, 2009, vol. 57 (6), pp. 1865–74.
12. M.G. Lee, G.D. Ko, J. Song, and K.J. Kang: *Mater. Sci. Eng. A*, 2012, vol. 539, pp. 185–93.
13. R.W. Fonda, M.J. Scherr, A.B. Geltmacher, and K.W. Sharp: *J. Mater. Eng. Perform.*, 2013, vol. 22 (11), pp. 3376–80.
14. W. Cai, X.L. Lu, and L.C. Zhao: *Mater. Sci. Eng. A*, 2005, vol. 394 (1–2), pp. 78–82.
15. H. Shi, S. Pourbabak, J.V. Humbeeck, and D. Schryvers: *Scripta Mater.*, 2012, vol. 67 (12), pp. 939–42.
16. A. Bansiddhi and D.C. Dunand: *J. Mater. Eng. Perform.*, 2011, vol. 20 (4), pp. 511–16.
17. A. Bansiddhi and D.C. Dunand: *Adv. Eng. Mater.*, 2011, vol. 13 (4), pp. 301–05.
18. M. Piao, S. Miyazaki, K. Otsuka, and N. Nishida: *Mater. Trans.*, 1992, vol. 33 (4), pp. 337–45.
19. W.C. Oliver and G.M. Pharr: *J. Mater. Res.*, 1992, vol. 7 (6), pp. 1564–83.
20. J.P. Micklich, C. Somsen, A. Dlouhy, C. Begau, A. Hartmaier, M.F. Wagner, and G. Eggeler: *Acta Mater.*, 2013, vol. 61 (2), pp. 602–16.